



Computer vision application programming for settlement monitoring in a drainage tunnel

I-Hui Chen^{a,*}, Shei-Chen Ho^b, Miao-Bin Su^a

^a Department of Civil Engineering, National Chung Hsing University, 145 Xingda Rd., South Dist., Taichung City 402, Taiwan

^b Cianshun Technology Co., LTD., 17 Yonghe 1st St., South Dist., Taichung City 402, Taiwan

ARTICLE INFO

Keywords:

Computer vision
Field monitoring
Settlement meter
Drainage tunnel

ABSTRACT

The study employs computer vision technology to pose a new type of optical instrument composed of the Raspberry Pi, digital cameras and chessboards for structural settlement monitoring. Using the OpenCV functions `findChessboardCorners` and `cornerSubPix`, displacement measurements in five distances between a camera and chessboard at 15, 17, 20, 23 and 25 m were undertaken to analyze measuring standard deviations that were from 0.027 to 0.048 pixels in laboratory tests. For field testing, five optical settlement instruments were installed at a drainage tunnel that was constructed at an 80-m-depth location within a landslide area. The resolution and accuracy of the instrument can be determined at 0.01 and 0.11 cm, respectively, as an optimally installed distance of 20 m in the drainage tunnel. The maximum settlement amount of field monitoring was 0.61 cm in six months. Overall, the optical instrument is more cost-effective and IOT-based for a long-term settlement monitoring.

1. Introduction

Computer vision was not accessible to the monitoring of civil engineering because it required a lot of heavy programming and processing in the past. Generally, conventional settlement gauges and theodolites are used for settlement measurement of structures [1,2]. However, these sensors are still complicated operation and time-consuming installation; in particular, measuring deformation for an underground structure in an alpine landslide area is unhandy and expensive using theodolites [3–6]. Other conventional sensors of displacement monitoring in landslides, such as GPS and extensometers, are still costly and difficult to monitor deformation of inside structure in alpine areas [7–9]. Computer vision technology has been used for a construction safety relevant to information from site images and videos compared to time-consuming and manually traditional practices [10–17].

Thus, the aim of the study is to pose a new monitoring instrument for potential structure deformation using computer vision technology which can automatically and economically detect settlement and displacement in a landslide area. The study employed computer vision technology with the OpenCV library to calculate image pixel changes of relative displacement between a chessboard and a digital camera connected to a device of the Raspberry Pi. The microcomputer Raspberry Pi is specifically designed to interact with sensors, motors, lights, and all

kinds of devices [18]. The Raspberry Pi can be easily used for computer vision applications to detect image changes of a chessboard relative to a digital camera that can take photos of a 3-by-3 chessboard target in which there are nine coordinate points using the OpenCV library [19–21]. Consequently, the study applied the instrument and the computer vision technology to analyze differences of image pixels if the chessboard moved.

Laboratory and filed tests were performed to practice feasibility of the optical settlement meter for settlement monitoring using the computer vision technology. Field testing involved displacement monitoring application of the optical settlement meter that was installed at an underground drainage tunnel within a landslide area for a long-term monitoring system.

2. Overview of computer vision techniques

Computer vision-based approaches can be mainly divided into object detection and action recognition, with chessboards and without a chessboard (so-called target object) using 2D- and 3D-image cameras, respectively. For object detection, a vision metrology of digital cameras was used for measuring tunnel deformation in X, Y and Z direction to analyze many mosaicked photos using many target objects [12]. Although the accurate of the vision metrology was similar to a total station instrument by 0.5 mm, the data was manually processed and

* Corresponding author.

E-mail address: cih82nchu@dragon.nchu.edu.tw (I.-H. Chen).

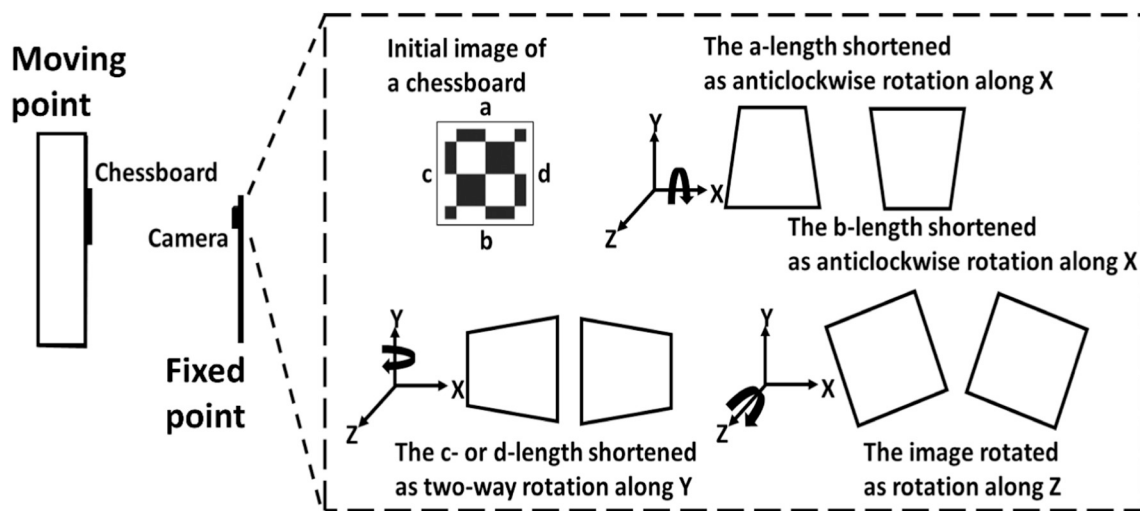


Fig. 1. Principle of calculating image changes.

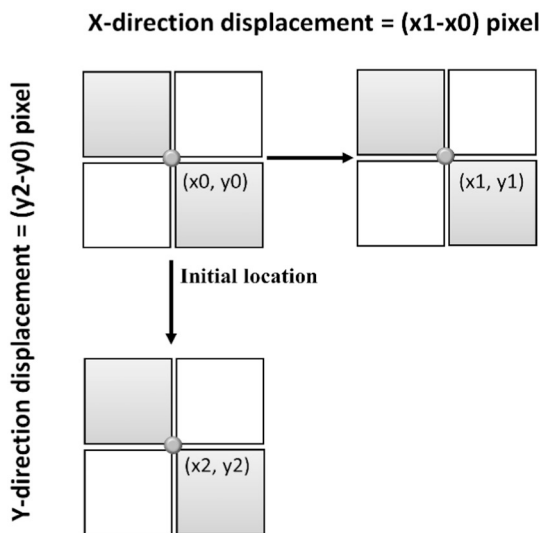


Fig. 2. Diagram of calculating image pixels for a chessboard movement.

analyzed. A vision-based system which remotely detected dynamic displacement of bridges using digital real-time image processing techniques with chessboards [13]; however, the system required an unhandy camcorder, laptop and specialized target recognition algorithm although its accuracy was less than 3% errors.

Technologies in computer vision have been applied to detect damage in monitored tunnel cracks using a cheap digital camera without chessboards so that areas with more severe damage were prioritized for monitoring [14]. However, it needed a specialized change detection algorithm that was applied to determine the change regions of bridge or tunnel inspection between query and reference images. Thus, it was still impractical for use with open-source programming from a general and public condition. A dynamic detection algorithm of slope gradient of locator based on computer vision technology was proposed to detect dynamically slope gradient of catenary locator using a corner matching algorithm [15]. Although the algorithm can automatically detect straight line angle in the locator slope without a chessboard, the resolution was one degree that could not be suitable for measuring resolution of civil engineering by arc seconds. A computer vision technique which measures three-dimensional deformations of a soil surface in a tunnel construction was presented using industrial cameras and was shown the overall accuracy within 0.05 mm in the laboratory [16]. Nevertheless, it was limited to a smaller scale and not employed for

field tests in spite of a computer vision-based system of high-density, accurate 3D point clouds.

A non-target computer vision-based method for displacement and vibration measurement was proposed using scale-invariant feature transform that was a kind of OpenCV functions [17]. To calculate the converting ratio between pixel-based displacement and engineering unit (millimeter), the maximum difference between the proposed computer vision-based method and electronic accelerometers is less than 5% [17]. Although the method was a simple, less complicated and more cost-effective system, it may be limited at high contrast, matching key points and no changing illumination, and cannot be real time for long-term monitoring and connected to internet as an IOT system.

Above the literature review, many computer vision-based devices and systems would still need to be improved. Thus, the goal and contribution of the study are to further improve displacement monitoring for a tunnel in a landslide area using the computer vision-based method with chessboards. Three contributions are proposed as follows: a) a new set of optical devices based on the computer vision technology, as called optical settlement meter, can replace conventional landslide monitoring device such as unhandy settlement gauges and costly theodolites; b) development of an automatic programming using open-source OpenCV can reach the resolution of the instrument for civil engineering-based monitoring displacements (millimeter); c) the optical settlement meter enables not only a more cost-effective and energy-saving monitoring method, but also a real-time and IOT-based system for a long-term settlement monitoring.

3. Method of laboratory testing

The principle of computer vision for settlement monitoring is to detect image distortion of a chessboard pattern fixed at an observing location. To calculate changes of image displacement at the observing location is relative to a digital camera installed at a fixed location, as shown in Fig. 1 which illustrates the deformation of three axes can cause image changes of the chessboard. If a moving point with a chessboard occurs settlement, relative image changes of a camera at a fixed point will be detected using the computer vision technology.

A 3-by-3 size of chessboard was detected every time in the image by a camera so that nine internal corner points on the chessboard were interpreted as reference coordinates by the image recognition of the OpenCV library in the study. The OpenCV functions findChessboardCorners and cornerSubPix can be used to locate corners of a chessboard [20,22–24]. The function findChessboardCorners in OpenCV calib3d module can automatically detect and sort nine corners at sub-pixel level in the 3 × 3 size of chessboard. Reference coordinates

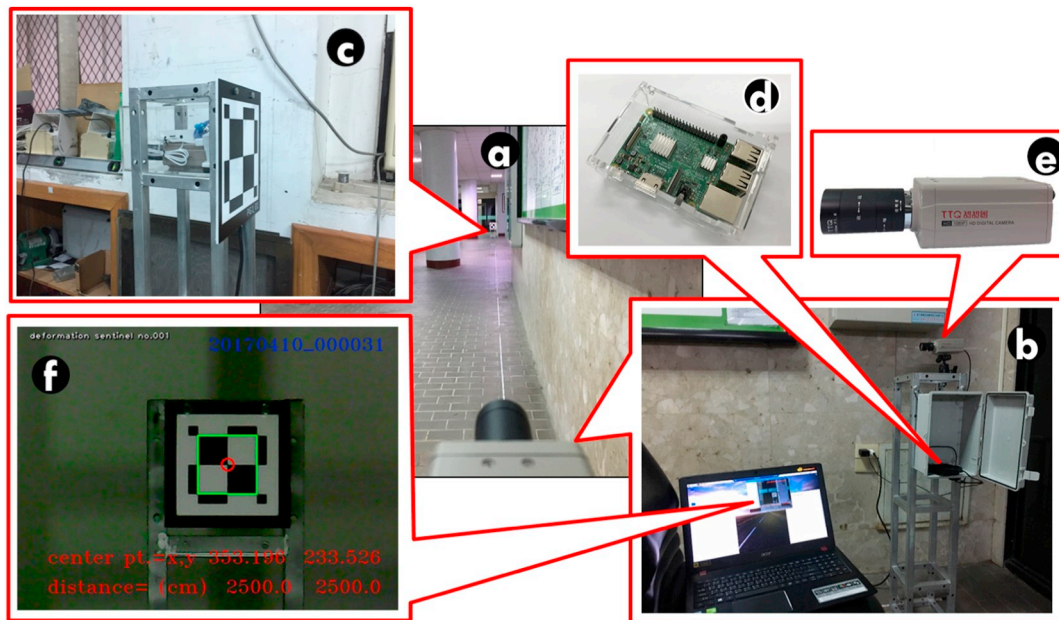


Fig. 3. Instrumentation of the optical settlement meter in the laboratory.

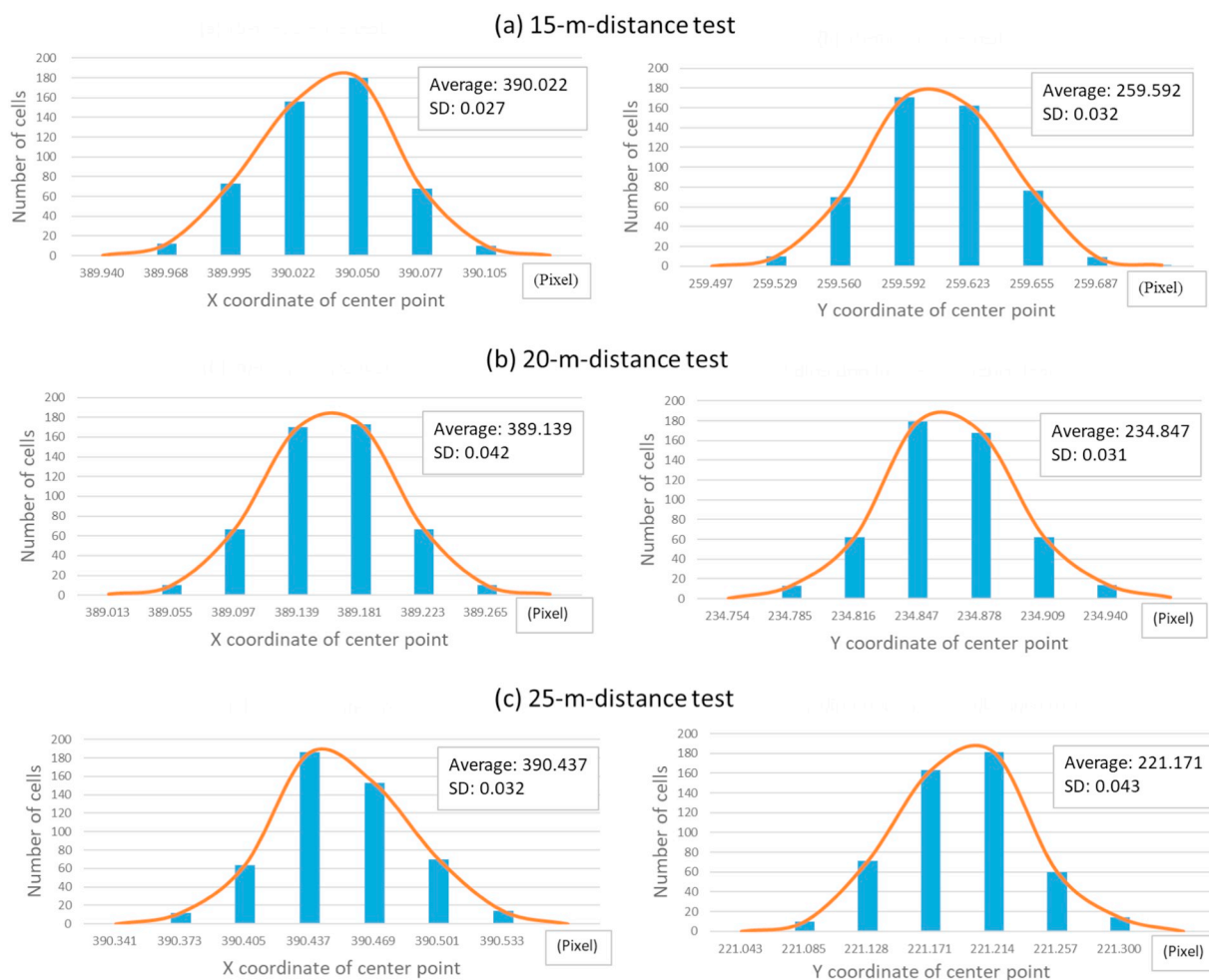


Fig. 4. Accuracy histograms of the center point of a chessboard in three distance testing. a) 15-m distance, b) 20-m distance and c) 25-m distance.

of the nine corners are calculated by the function `cornerSubPix` in OpenCV `imgproc` module which adopts an iterative strategy to find the accurate sub-pixel location of corners after obtaining corners by the

function `findChessboardCorners` using the algorithm of a Hessian corner detector [19,25].

Using the OpenCV functions, pixel changes of chessboard images

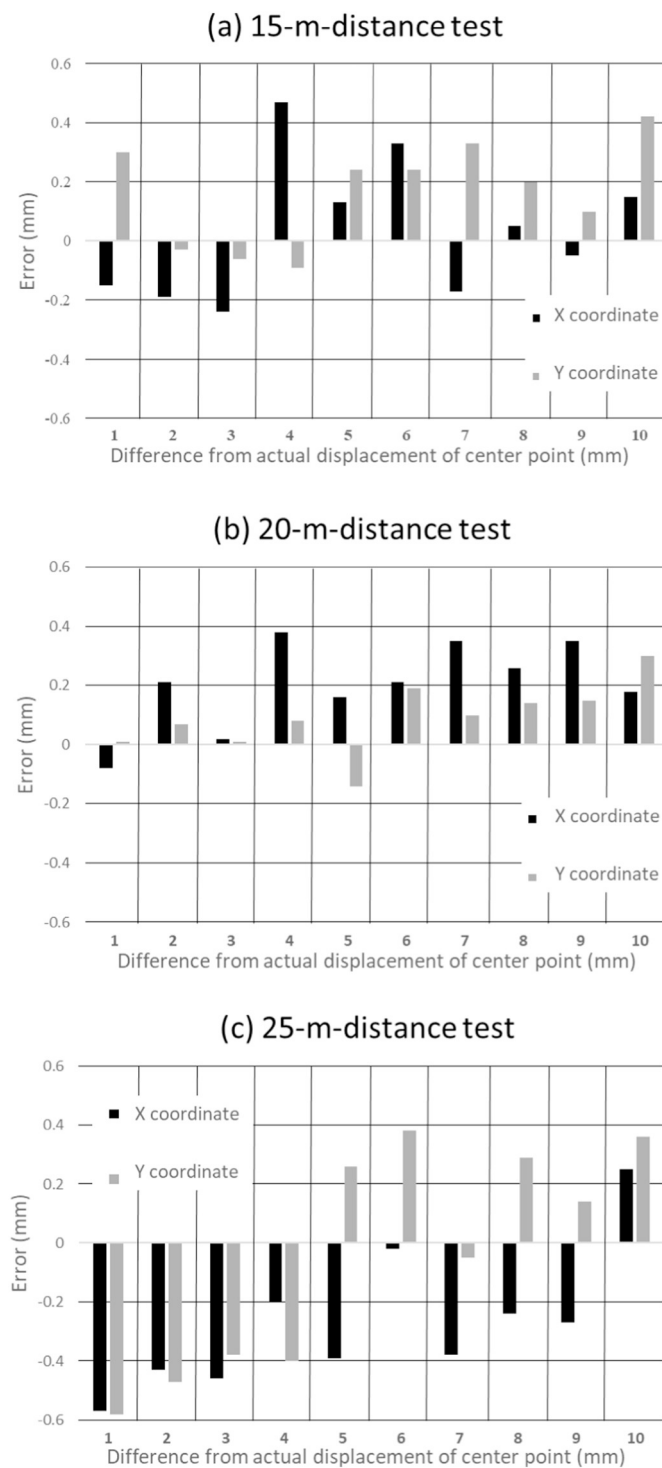


Fig. 5. Errors of different displacements in the center point of a chessboard for three distance testing. a) 15-m distance, b) 20-m distance and c) 25-m distance.

can be automatically recognized to calculate physic displacements. For example, x and y coordinates of the center point on the chessboard can be compared to differences from their displacements if the chessboard was moved from x_0 to x_1 or from y_0 to y_2 corresponding to x-direction or y-direction displacement, respectively, as shown in Fig. 2. Thus, relative settlement measuring can be determined according to changes of the y-direction displacement through the OpenCV application in the study.

Instrumentation of an optical settlement meter in the laboratory is mainly composited of a digital camera and the Raspberry Pi 3 fixed at a

steel frame, and a chessboard fixed at another steel frame (Fig. 3). The devices of the optical settlement meter include two main units which were set up at two locations in distances from 15 to 25 m to undertake laboratory tests for determining an optimally installed distance of the optical settlement meter in Fig. 3(a). The first unit is a steel frame in 100-cm length and 20-cm width as shown in Fig. 3(b) and the other unit is another steel frame with a 15-by-15-cm chessboard in Fig. 3(c). The first unit consists a set of the Raspberry Pi (Fig. 3(d)) and a digital camera with 640×480 resolution (Fig. 3(e)). The study designed self-programming with Python to calculate image pixel values of chessboard's corner points that were recognized as an image in a green rectangle line for a perimeter on the chessboard and another image in a red circle for a center point on it, as shown in Fig. 3(f).

For instance, image pixel values of the center point in x and y coordinate in Fig. 3(f) were 353.196 and 233.526 pixels, respectively. If the chessboard in Fig. 3(f) moved or subsided, changes in the image pixel value would be automatically detected using the OpenCV library with the Python programming.

Converting a pixel unit to centimeters, a physical displacement can be calculated using a focal-length equation ($D = f \times X \div x$) where D means a distance between a camera and a chessboard; f is a fixed focal length; X means a physical x-direction length of a chessboard pattern and x means pixel values of chessboard's x-direction length on the imaging plane [19,22,23]. For example, the sum of coordinate pixels in four corners of the chessboard displayed as green line in Fig. 3(f) was 146.341 pixels when the physical perimeter in the 15-by-15-cm chessboard was 60 cm, so the relationship involves that 1 pixel equaled 0.41 cm for the 25-m-distance test in the study. In other words, if the image of chessboard is detected as a one-pixel movement downward in y direction for the 25-m-distance test, it means that the relative chessboard is subsided at 0.41 cm.

Two kinds of laboratory tests were performed to detect image recognition of a chessboard in the optical settlement meter. The first is that five distances between the camera and the chessboard at 15, 17, 20, 23 and 25 m were undertaken to determine optimally installed distance which should be considered on measuring errors of the optical settlement meter and feasibility of field installation. The other laboratory test was performed to simulate displacement of the chessboard in the optical settlement meter using a STAGE manual fine adjustment platform whose movements from 1 to 10 mm were manually controlled and recorded.

For examples of the distance testing in 15, 20 and 25 m, Fig. 4 shows accuracy histograms for the three distance observations whose total number of cells is 500 in x direction, y direction of the center point of a chessboard, respectively. The coordinate and standard deviation of center point in the x and y directions were 390.022 and 0.027 pixels, and 259.592 and 0.031 pixels, respectively, for the 15-m distance testing in Fig. 4(a). The standard deviations of center points in the x and y directions for the 20- and 25-m tests were 0.042 and 0.031 pixels, and 0.032 and 0.043 pixels, respectively, in Fig. 4(b) and (c). To convert a pixel unit to centimeters for all tests is discussed later.

For the other laboratory testing, different displacements of the x and y direction in a chessboard were set at a given value from 1 to 10 mm. For instance, Fig. 5 shows average errors of measuring for different displacements from 1 to 10 mm in x direction, y direction of the center point of a chessboard for 15-, 20- and 25-m distance tests, at 0.19, 0.21 and 0.30 mm, respectively. Above the two laboratory tests, an optimal distance between a camera and chessboard, and the resolution and accuracy of the optical settlement meter can be determined, as discussed later.

Finally, the instrument of similar laboratory testing was installed at a drainage tunnel which was constructed at the 80-m-depth location in a landslide area in order to monitor potential settlement of the underground structure. A tendency of settlement changes can be measured through long-term monitoring of the optical settlement meter in the field.

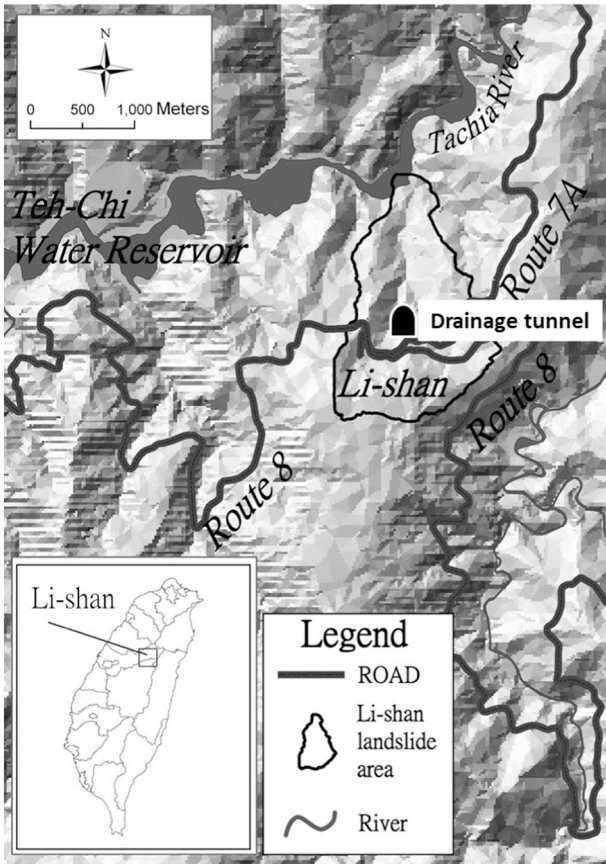


Fig. 6. Location of the drainage tunnel in Lishan landslide area.

4. Field testing in a drainage tunnel

The drainage tunnel is located at Lishan landslide area in central Taiwan, as shown in Fig. 6. The area occurred a severe landslide after prolonged torrential rainfall in April 1990. For remediation of the landslide, a drainage tunnel (No. G1) with 350 m in length was constructed at an 80-m-depth location within the landslide area to discharge deep groundwater against landslides. When constructed the

drainage tunnel from 1999 to 2001, several locations in distance between 185 and 280 m from its entrance had occurred seepage and collapse, where there exit more weathered and broken stratum [26]. Thus, it is a vital for landslide monitoring to observe potential deformation of the drainage tunnel. Five optical settlement meters were installed at locations from 190 to 290 m at the interval of 20 m to monitor the displacement and settlement of the section in the drainage tunnel in 2018. The interval was determined through an optimal condition of the laboratory testing as discussed later.

The five optical settlement meters (S1–S5) were installed at G1 drainage tunnel as shown in Fig. 7. Fig. 7(a) illustrates the profile graph of the drainage tunnel where there are six steel frames at locations from 190 to 290 m for the five optical settlement meters. Each optical settlement meter has two steel frames (one is for the installation of a camera and the Raspberry Pi; the other is for the installation of a relative chessboard). As displayed in Fig. 7(b), a configuration of the optical settlement meter S1 includes two steel frames at the interval of 20 m within the drainage tunnel. Fig. 7(c) shows finished instrumentation of S1 that is composed of the Raspberry Pi, a digital camera and a steel frame. Meanwhile, the other frame was installed at 20-m-interval location including not only a relative chessboard of S1 but also the Raspberry Pi and the digital camera of S2 (see Fig. 7(d)). The same kind of the two steel frames was installed at the S3, S4 and S5 configurations. Finally, there is only a relative chessboard of S5 in the last steel frame shown in Fig. 7(e).

All field monitoring data of these optical settlement meters was recorded using image resolution of 640×480 pixels captured at a rate of one frame per 10 min. The Python programming was designed to automatically interpret pixel changes in the chessboard of the optical settlement meter. Furthermore, image pixel values were recoded as a file in the Raspberry Pi which can transmit the file to FTP cloud system as an IOT system in real time.

Graphs of the monitoring data of the five optical settlement meters from Jan/2018 to Jun/2018 were presented in Fig. 6 where left vertical axis means pixel changes in x coordinate of the center point on the chessboard and right vertical axis means pixel changes in y coordinate of the center point on it. Using the computer vision technology, pixel changes in the center point on the relative chessboard of the optical settlement meter can be detected as displacement change monitoring. X-coordinate pixel changes present relative displacement of the chessboard in a horizontal direction. Also, y-coordinate pixel changes show

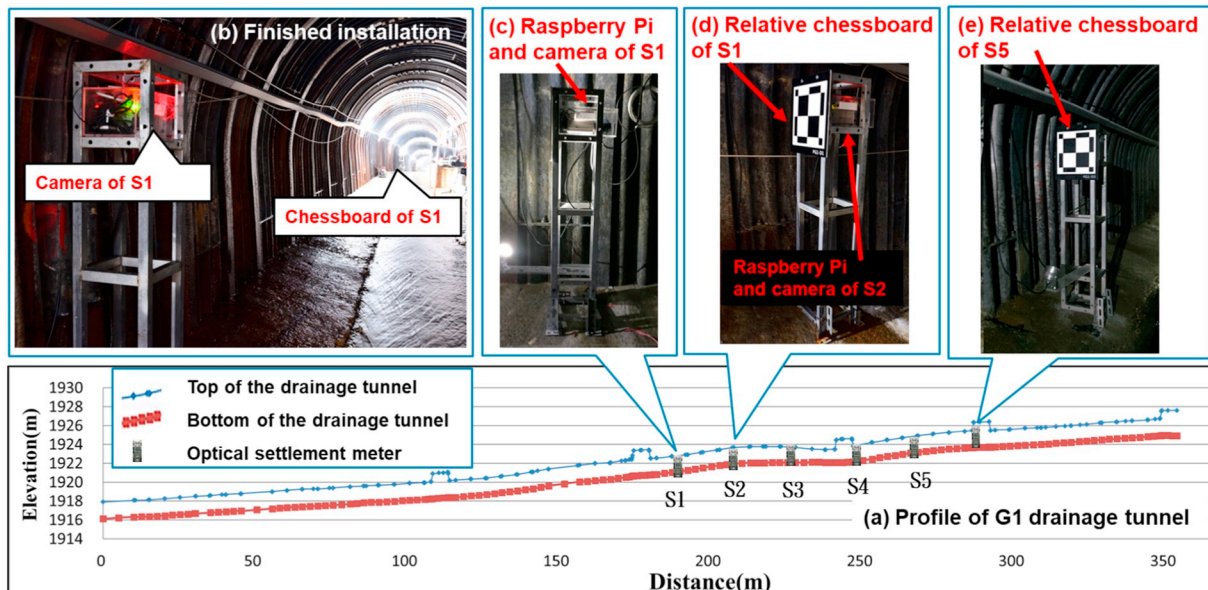


Fig. 7. Configuration of the optical settlement meter in the drainage tunnel.

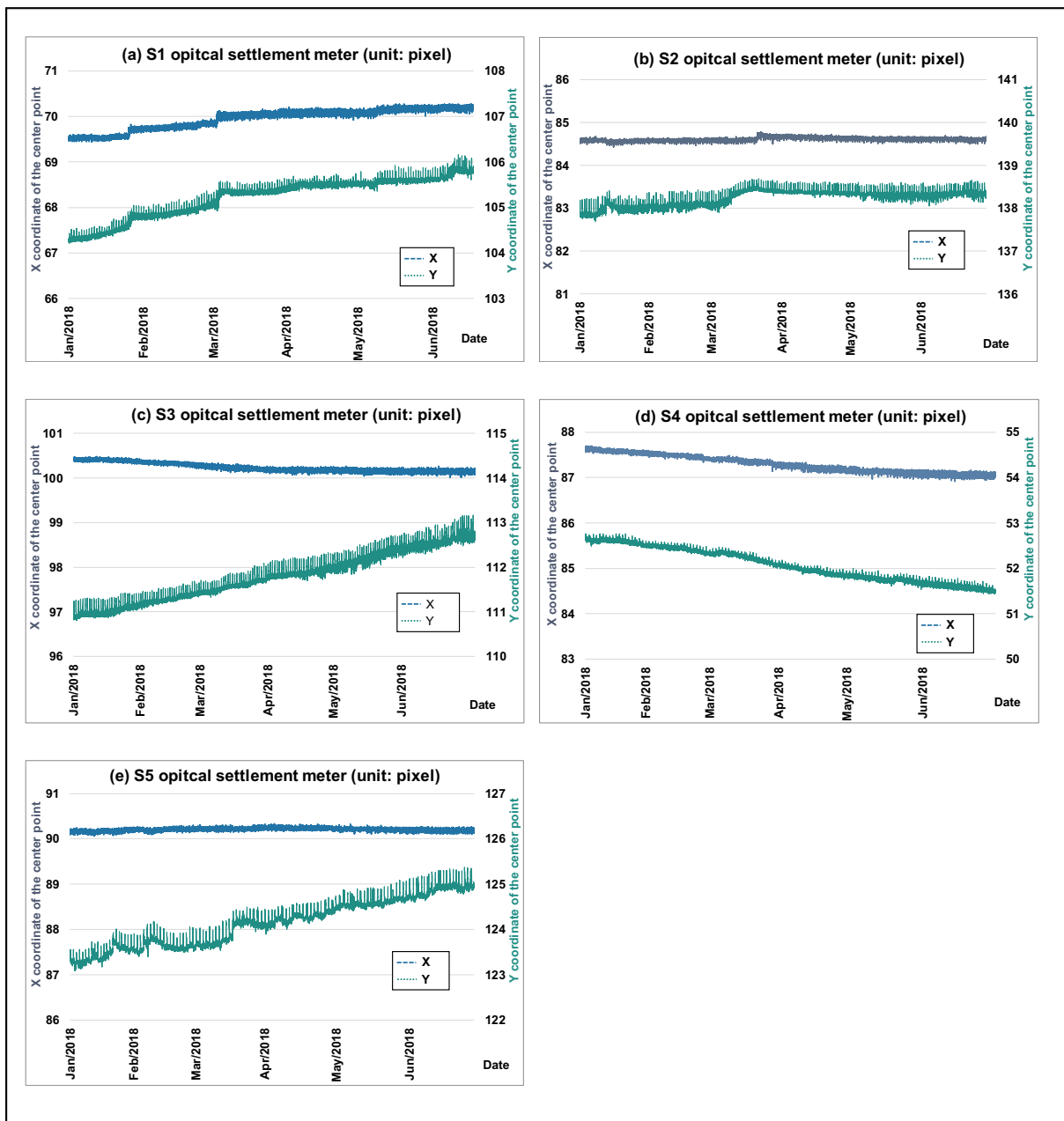


Fig. 8. Graph of monitoring data from the S1 settlement meter in the drainage tunnel.

Table 1
Testing of chessboard images in different distances between a camera and chessboard.

Distance	Length per pixel in the chessboard image (cm)	Center point of chessboard	Standard deviation (pixel)	Average standard deviation (cm)
15 m	0.26	X coordinate	0.027	0.01
		Y coordinate	0.032	
17 m	0.29	X coordinate	0.028	0.01
		Y coordinate	0.038	
20 m	0.34	X coordinate	0.042	0.01
		Y coordinate	0.031	
23 m	0.38	X coordinate	0.041	0.02
		Y coordinate	0.042	
25 m	0.41	X coordinate	0.032	0.02
		Y coordinate	0.043	

relative settlement of the chessboard in a vertical direction. For example, Fig. 8(a) shows the monitoring data from the S1 optical settlement meter where there was a slight increase change in x coordinate of the chessboard from approximately 69.5 to 70 pixels. It means that the chessboard of S1 was left moved in horizontal direction by approximately 0.5 pixels relative to the camera of S1 from Jan/2018 to Jun/2018. Also, pixel changes in y coordinate of the chessboard significantly rose from approximately 104 to 106 pixels, which showed the chessboard of S1 was dramatically subsided in vertical direction in the period.

Furthermore, errors of the y-coordinate pixel changes fluctuated more dramatically between 0 and 0.33 pixels than the x coordinate between 0 and 0.18 pixels in the S2 optical settlement meter (see Fig. 8(a)). For the S2 optical settlement meter, x- and y-coordinate pixels slightly changed as shown in Fig. 8(b). Errors of the y-coordinate pixel changes in S2 fluctuated between 0 and 0.35 pixels. On the other hand, there were significant relative settlement changes of y-coordinate

Table 2
Measurement of image change in x- and y-axis movement of chessboard.

Actual movements (mm)	X direction		Y direction	
	Measuring movements (mm)	Error (mm)	Measuring movements (mm)	Error (mm)
1	0.92	0.08	1.11	0.11
2	2.21	0.21	2.17	0.17
3	3.02	0.02	3.01	0.01
4	4.38	0.38	4.07	0.07
5	5.16	0.16	4.76	0.24
6	6.21	0.21	6.19	0.19
7	7.35	0.35	7.10	0.10
8	8.26	0.26	8.12	0.12
9	9.35	0.35	9.15	0.15
10	10.18	0.18	10.20	0.20

pixels in S3, S4 and S5 as shown in Fig. 8(c)–(e). Maximum errors of the pixel fluctuations in S3, S4 and S5 were 0.31, 0.26 and 0.30 pixels, respectively.

Through laboratory and field testing, the study can discuss and determine the resolution and accuracy of the optical settlement meter which was employed for the settlement monitoring of the drainage tunnel in the landslide area.

5. Result and discussion

For laboratory tests, five distances between the camera and the chessboard of the optical settlement meter at 15, 17, 20, 23, and 25 m were performed to determine an optimally installed distance using the computer vision technology. Results of the laboratory testing are shown in Table 1 which presents average standard deviations of 0.01 and 0.02 cm. Although shorter distance presented a better standard deviation of image pixels in the optical settlement meter, the 20-m distance was also the same average standard deviation of 0.01 cm as the 15-m distance. However, there was a worse average standard deviation in the distance greater than 20 m by 0.02 cm. Thus, the optimally installed distance can be determined as 20 m. That was why that field installed distance was at the interval of 20 m in the drainage tunnel.

For the other laboratory testing, different displacements of the x- and y-axis direction from 1 to 10 mm were carried out in the 20-m distance between the camera and the chessboard. Table 2 shows the result of the x- and y-coordinate movement tests. From Table 2, errors of x- and y-coordinate changes were from 0.02 to 0.38 mm. Average errors of the x- and y-coordinate changes were approximately 0.22 mm and 0.14 mm, respectively.

Thus, the resolution of the optical settlement meter can be determined as 0.01 cm because the average standard deviation of the laboratory testing in Table 1 was 0.014 cm. Furthermore, the maximum error of the laboratory testing in Table 2 was 0.38 mm (0.04 cm) that

seems to be an accuracy of the optical settlement meter. However, results of field testing must be considered as the determination of the accuracy in the optical settlement meter.

For field testing in the drainage tunnel, the monitoring data from five optical settlement meters (S1–S5) was automatically recorded between Jan/2018 and Jun/2018. As aforementioned above, graphs of the monitoring data were presented in Fig. 8(a)–(e). There exists no significant displacement of the center points on the chessboards of S2. However, graphs of the S1, S3, S4 and S5 monitoring data illustrated that there were significant changes upward and downward in x- and y-coordinate pixels of center points on their relative chessboards. For recognition of the changes in a tendency, the method of moving average was used to smooth the time series and to find the tendency over time [27,28]. Thus, 1-day moving average of field monitoring data was used to show a trend of settlement changes in the study. The optical settlement meter was originally recorded every 10 min so 144-term moving average means one point of monitoring data per day. Results of the moving average were shown in Fig. 9 which illustrated the tendency of the settlement monitoring every day for S2 and S3 from Jan/2018 to Jun/2018. Fig. 9(a) shows the smaller amount of settlement monitoring in S2 from Jan/2018 to Jun/2018 was approximately 0.5 pixels. However, there was a maximum relative settlement change in S3 among the five optical settlement meters from 110.89 to 112.69 pixels in the period (Fig. 9(b)).

The amount of relative settlement every optical settlement meter in the drainage tunnel can be measured using the method of the moving average. Accumulative settlement changes in the five optical settlement meters and their errors were presented in Table 3. The changes in the y-direction pixel of S1 gradually increased by 1.54 pixels. It means that the relative chessboard gradually subsided at 0.52 cm in the period (1 pixel equals 0.34 cm in the 20-m-distance installation of the optical settlement meter in Table 1). Meanwhile, the data from the S1 settlement monitoring was plotted in Fig. 8(a), which shows there was an error fluctuation of measuring pixels at the range of average 0.33 pixels, so average error was approximately 0.11 cm (see Table 3). However, it was interesting for S4 that sum of settlement changes from Jan/2018 to Jun/2018 was -1.15 pixels (see Fig. 8(d) and Table 3). It means the relative camera in S4 occurred settlement so that the relative chessboard of S4 seemed become upward. It can be proved that the camera of S4 was installed at the back of the chessboard of S3 where there was a maximum settlement change by 1.8 pixels corresponding to the settlement amount of 0.61 cm. Table 3 also presents that errors of the field testing range from 0.26 to 0.35 pixels and average error of the settlement amount is 0.11 cm that can be regarded as the accuracy of the optical settlement meter in the field.

Through laboratory and field tests, the resolution of the optical instrument was 0.01 cm in the laboratory while the accuracy of the case study in the field was 0.11 cm. As a result, the optical settlement meter was practicable and feasible for displacement monitoring in the

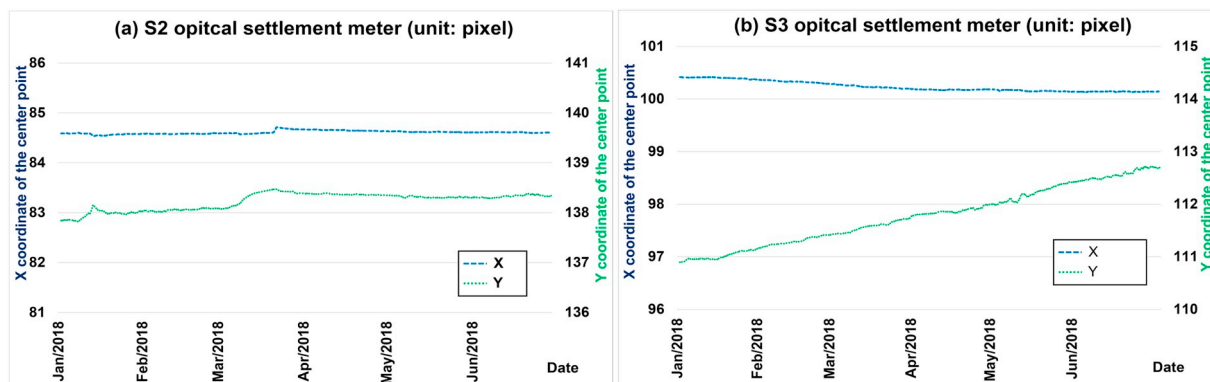


Fig. 9. 1-day moving average of x- and y-coordinate pixel changes in the S2 and S3 optical settlement meters.

Table 3

Accumulative values of settlement monitoring for field testing from Jan/2018 to Jun/2018.

Code	Sum of settlement change (pixel)	Sum of settlement amount (cm)	Error of Settlement changes (pixel)	Error of Settlement amount (cm)
S1	1.54	0.52	0.33	0.11
S2	0.50	0.17	0.35	0.12
S3	1.80	0.61	0.31	0.11
S4	-1.15	-0.39	0.26	0.09
S5	1.64	0.56	0.30	0.10

Table 4

Comparison of the optical settlement meter and traditional monitoring devices.

	Optical settlement meter	Liquid settlement gauge	Total station theodolite
Resolution	0.1 mm	0.2–0.5 mm	0.1 mm
Price	\$150 USD	\$1000 USD	\$10,000 USD
IOT application	Yes	Yes, if connected communication networks	Yes

underground structure over a long period of time. Finally, an optical settlement meter based on IOT system costs approximately \$150 USD that is cost-effective for the settlement measuring of the underground structure in the landslide area.

Comparing to conventional monitoring devices such as liquid settlement gauges and total station theodolites, Table 4 presents the resolution and price of the optical settlement meter and the two traditional devices. Liquid settlement gauges are based on the principle of hydraulic pressure in a full-sealed system to transform to the amount of ground settlement [29]. Tunnel deformation monitoring are often detected using total station theodolites which can be automatically worked to measure reliable data with prisms [30]. From Table 4, the optical settlement meter based on IOT system costs much cheaper than traditional monitoring devices while its resolution is similar to those.

6. Conclusion

The study posed a computer vision-based instrument to monitor settlement for an underground structure within a landslide area. The optical settlement meter was composed of the Raspberry Pi, a digital camera and a chessboard target. For laboratory testing, the optimally installed distance between the camera and relative chessboard in the optical settlement meter was 20 m. For field testing, five optical settlement meters were installed at the drainage tunnel in Lishan landslide area to monitor displacement of the underground structure in real time. From Jan/2018 to Jun/2018, the monitoring data from the five optical settlement meters (S1–S5) illustrated that maximum settlement amount was 0.61 cm in S3. For the other optical settlement meters, there were also significant changes in S1, S4 and S5. Through the laboratory and field testing, the resolution and accuracy of the optical settlement meter can be determined as 0.01 and 0.11 cm, respectively. However, there are some limitations of the optical settlement meter: a) it needs enough fill light so the study uses the highest intensity of LED lights in the field. b) all optical devices are often affected by environmental temperature. Nevertheless, the temperature maintains approximately 24 °C all year in the underground structure so the result of the field testing is not influenced by the temperature.

Overall, the optical settlement meter based on the computer vision application costs much cheaper than traditional settlement-monitoring devices. Using the optical settlement meter, the settlement and displacement monitoring of the drainage tunnel can be detected as an automatic and economical IOT system in the landslide area for a long

period. In the future, it would replace these traditional monitoring devices and could be an early warning system if a landslide occurs seriously settlement.

Declaration of competing interest

All authors have participated in (a) conception and design, or analysis and interpretation of the data; (b) drafting the article or revising it critically for important intellectual content; and (c) approval of the final version.

This manuscript has not been submitted to, nor is under review at, another journal or other publishing venue.

The authors have no affiliation with any organization with a direct or indirect financial interest in the subject matter discussed in the manuscript.

Acknowledgments

Field testing in the study could be realized through the support and sponsorship of the Soil and Water Conservation Bureau, Council of Agriculture, Executive Yuan, Taiwan. Consecutive projects including long-term monitoring are proposed and approved by the technical counselling committee on the remediation works of the Lishan landslide area. Moreover, the performance evaluation of each project is periodically reviewed by the committee annually.

References

- [1] R.E. Hunt, *Geotechnical Investigation Methods: A Field Guide for Geotechnical Engineers*, CRC/Taylor & Francis, Boca Raton, FL, 2007.
- [2] J. Dunnycliff, *Geotechnical Instrumentation for Monitoring Field Performance*, Wiley, New York, 1988.
- [3] C.C. Lai, H.Y. Au, M.S. Liu, S.L. Ho, H.Y. Tam, Development of level sensors based on fiber Bragg grating for railway track differential settlement measurement, *IEEE Sensors J.* 16 (16) (2016) 6346–6350, <https://doi.org/10.1109/JSEN.2016.2574622>.
- [4] M. V. Ramesh, N. Vasudevan, The deployment of deep-earth sensor probes for landslide detection, *Landslides* 9 (4) (2012) 457–474, <https://doi.org/10.1007/s10346-011-0300-x>.
- [5] T. Uchimura, I. Towhata, L. Wang, S. Nishie, H. Yamaguchi, I. Seko, et al., Precaution and early warning of surface failure of slopes using tilt sensors, *Soils Found.* 55 (5) (2015) 1086–1099, <https://doi.org/10.1016/j.sandf.2015.09.010>.
- [6] S. Uhlemann, A. Smith, J. Chambers, N. Dixon, T. Dijkstra, E. Haslam, et al., Assessment of ground-based monitoring techniques applied to landslide investigations, *Geomorphology* 253 (2016) 438–451, <https://doi.org/10.1016/j.geomorph.2015.10.027>.
- [7] M.B. Su, I.H. Chen, C.H. Liao, Using TDR cables and GPS for landslide monitoring in high mountain area, *J. Geotech. Geoenviron.* 135 (8) (2009) 1113–1121, [https://doi.org/10.1061/\(ASCE\)GT.1943-5606.0000074](https://doi.org/10.1061/(ASCE)GT.1943-5606.0000074).
- [8] J.P. Malet, O. Maquaire, E. Calais, The use of global positioning system techniques for the continuous monitoring of landslides: application to the Super-Sauze earth-flow (Alpes-de-Haute-Provence, France), *Geomorphology* 43 (2002) 33–54, [https://doi.org/10.1016/S0169-555X\(01\)00098-8](https://doi.org/10.1016/S0169-555X(01)00098-8).
- [9] A. Corsini, A. Pasuto, M. Soldati, A. Zannoni, Field monitoring of the Corvara landslide (Dolomites, Italy) and its relevance for hazard assessment, *Geomorphology* 66 (2005) 149–165, <https://doi.org/10.1016/j.geomorph.2004.09.012>.
- [10] J. Seo, S. Han, S. Lee, H. Kim, Computer vision techniques for construction safety and health monitoring, *Adv. Eng. Inform.* 29 (2) (2015) 239–251, <https://doi.org/10.1016/j.aei.2015.02.001>.
- [11] H. Luo, C. Xiong, W. Fang, P.E. Love, B. Zhang, X. Ouyang, Convolutional neural networks: computer vision-based workforce activity assessment in construction, *Autom. Constr.* 94 (2018) 282–289, <https://doi.org/10.1016/j.autcon.2018.06.007>.
- [12] S. Miura, T. Yamamoto, I. Kuronuma, M. Imai, Vision metrology applied for configuration and displacement, *International Journal of the JCRM* 1 (2005) 1–6, <https://doi.org/10.11187/ijjcr.1.1>.
- [13] J.J. Lee, M. Shinozuka, A vision-based system for remote sensing of bridge displacement, *NDT & E International* 39 (2006) 425–431, <https://doi.org/10.1016/j.ndteint.2005.12.003>.
- [14] K. Chaiyasarn, *Damage Detection and Monitoring for Tunnel Inspection Based on Computer Vision* University of Cambridge, (2014), <https://doi.org/10.17863/CAM.14071>.
- [15] T. Zhang, K.S. HAO, R. Duan, Dynamic detection algorithm of slope gradient of catenary locator based on computer vision technology, *Railway Standard Design* 1 (2013) 105–108, <https://doi.org/10.13238/j.issn.1004-2954.2013.01.001>.
- [16] B.T. Le, S. Nadimi, R.J. Goodey, R.N. Taylor, System to measure three-dimensional

- movements in physical models, *Géotechnique Letters* 6 (2016) 1–7, <https://doi.org/10.1680/jgele.16.00073>.
- [17] T. Khuc, F.N. Catbas, Computer vision-based displacement and vibration monitoring without using physical target on structures, *Struct. Infrastruct. Eng.* 13 (2017) 505–516, <https://doi.org/10.1080/15732479.2016.1164729>.
- [18] J. Cicolani, *Beginning Robotics With Raspberry Pi and Arduino: Using Python and OpenCV*, Apress, 9781484234624, 2018.
- [19] A. Kaehler, G. Bradskia, *Learning OpenCV: Computer Vision With the OpenCV Library*, O'Reilly Media, Inc, 2008.
- [20] OpenCV Team, OpenCV API Reference, <https://docs.opencv.org/3.1.0/>, (2014) (Accessed date: Marche 2017).
- [21] GitHub Inc, Open Source Computer Vision Library, <https://github.com/opencv/opencv/tree/3.1.0>, (2016) (Accessed date: March 2017).
- [22] Z. Zhang, A flexible new technique for camera calibration, *IEEE Trans. Pattern Anal. Mach. Intell.* 22 (2000) 1330–1334, <https://doi.org/10.1109/34.888718>.
- [23] T. Luhmann, S. Robson, S. Kyle, I. Harley, *Close Range Photogrammetry*, Wiley, 2007.
- [24] P. Ahmmed, Z. Ahmed, M.I.J. Rafee, M.A. Awal, S.M. Choudhury, Self-localization of a mobilerobot using monocular vision of a chessboard pattern, in: *IEEE (Ed.)*, 8th InternationalConference on Electrical and Computer Engineering, IEEE, Dhaka, Bangladesh, 2014, pp. 753–756, , <https://doi.org/10.1109/icece.2014.7026828>.
- [25] Y. Liu, S. Liu, Z. Wang, Y. Cao, Automatic chessboard corner detection method, *IET Image Process.* 10 (1) (2016) 16–23, <https://doi.org/10.1049/iet-ipr.2015.0126>.
- [26] D.G. Lin, S.H. Hung, C.Y. Ku, H.C. Chan, Evaluating the Efficiency of Subsurface Drainages for Li-Shan Landslide in Taiwan, *Natural Hazards and Earth System Sciences*, 2016, <https://doi.org/10.5194/nhess-2015-309> Discuss.
- [27] L. Nelson, The deceptiveness of moving averages, *J. Qual. Technol.* 15 (2) (1983) 99–100, <https://doi.org/10.1080/00224065.1983.11978852>.
- [28] C. Li, T.M. Fernández-Steeger, J.A.B. Link, M. May, R. Azzam, Use of MEMS accelerometers/inclinometers as a geotechnical monitoring method for ground subsidence, *Acta Geodyn. Geomater.* 11 (4) (2014) 337–349, <https://doi.org/10.13168/AGG.2014.0015>.
- [29] Y. Cui, Development status and prospect of deformation monitoring techniques for high-speed rails, 2017 2nd International Conference on Machinery, Electronics and Control Simulation (MECS 2017), Atlantis Press, 2016, , <https://doi.org/10.2991/mecs-17.2017.161>.
- [30] Leica Geosystems, Leica Geosystems TruStories Monitoring, <https://leica-geosystems.com/>, (2015) (Accessed date: December 2015).